



# Mechanism of Placenta Damage in Gestational Diabetes Mellitus by Investigating TXNIP of Patient Samples and Gene Functional Research in Cell Line

Sarina · Dong Fang Li · Zong Qi Feng · Jie Du · Wen Hua Zhao ·  
Na Huang · Jian Chao Jia · Zhou Ying Wu · Alamusi ·  
Yong Yun Wang · Xiao Li Ji · Lan Yu

Received: August 8, 2019 / Published online: October 26, 2019  
© The Author(s) 2019

## ABSTRACT

**Introduction:** Gestational diabetes mellitus (GDM) is a gestational complication that affects maternal and child health. The placenta provides the fetus with the necessary nutrition and oxygen and takes away the metabolic waste. Patients with GDM are diagnosed and treated merely on the basis of the blood glucose level; this approach does nothing to help evaluate the status of the placenta, which is worth noting in GDM. The purpose of this research was to clarify the relation between thioredoxin-interacting protein (TXNIP) and reactive oxygen species (ROS) in the placenta of patients with GDM, which has thus far remained unclear.

**Enhanced Digital Features** To view enhanced digital features for this article go to <https://doi.org/10.6084/m9.figshare.9944426>.

Sarina · D. F. Li · Z. Q. Feng · N. Huang ·  
J. C. Jia · Z. Y. Wu · Y. Y. Wang · X. L. Ji · L. Yu (✉)  
Department of Clinical Medical Research Center,  
Inner Mongolia People's Hospital, Hohhot 010010,  
China  
e-mail: cmrc123@hotmail.com

J. Du · W. H. Zhao  
Department of Gynecology and Obstetrics, Inner  
Mongolia People's Hospital, Hohhot 010010, China

Alamusi  
Department of Ophthalmology, Inner Mongolia  
International Mongolian Hospital, Hohhot 010000,  
China

**Methods:** The expression of TXNIP in the placentas of 10 patients with GDM and 10 healthy puerperae (control group) was investigated via immunofluorescence. The relation among TXNIP, ROS, and the function of mitochondria was explored in HTR-8/SVneo cells stimulated by high glucose (HG).

**Results:** The results showed the expression of TXNIP in the placentas of patients with GDM was higher than that in the control group, and the expression of TXNIP in HTR-8/SVneo cells treated with HG was higher than that in the control group, causing the accumulation of ROS and changes of mitochondria, promoting apoptosis and inhibition of migration.

**Conclusions:** High expression of TXNIP caused by HG mediates the increasing ROS and the mitochondria dysfunction in GDM; this impairs the function of the placenta and is the basis for the prediction of perinatal outcome.

**Keywords:** GDM; Mitochondria; Placenta; ROS; TXNIP

## Key Summary Points

### Why carry out this study?

The incidence of gestational diabetes mellitus (GDM) is increasing worldwide, especially in older pregnant women and overweight women. In China, as a result of the two-child policy, the number of elderly pregnant women with GDM is increasing year by year. Few studies have been conducted on the prediction of perinatal outcomes of pregnant women and fetuses. Our study on the development and function of the placenta, an important organ during pregnancy, provides some help for the prediction of perinatal outcomes.

We hope that our study can provide some references for the perinatal outcome of pregnant women with GDM, and predict the development and functional status of the placenta through the expression of specific proteins such as thioredoxin-interacting protein (TXNIP).

### What was learned from the study?

The study reveals the molecular mechanism of placental damage in GDM, which can also be applied to the prediction of perinatal outcomes. The expression of TXNIP increased significantly in the placentas of patients with GDM. When TXNIP was highly expressed in HTR-8 cells stimulated by high glucose (HG), the mitochondrial function was decreased, the accumulation of reactive oxygen species (ROS) and the increase of apoptosis were observed, and the proliferation and migration ability of the cells was impeded. Therefore, TXNIP plays an important role in the metabolism of the placenta in patients with GDM and participates in GDM placental dysfunction via increasing ROS and mitochondria dysfunction. The results will provide the basis for new methods of detecting placental function and for future interventions.

The expression of TXNIP in the placentas of patients with GDM was significantly increased compared with normal pregnancy. High expression of TXNIP leads to inhibition of cell proliferation, increase of apoptosis and inhibition of cell migration, and occurrence of mitochondrial apoptosis. These changes may be related to the accumulation of cellular oxidative stress induced by TXNIP. Therefore, in this study, TXNIP plays a very important role in the placental development of patients with GDM.

High expression of TXNIP caused by HG mediates the increasing ROS and the mitochondria dysfunction in GDM, proving the basis for the prediction of perinatal outcome.

## INTRODUCTION

Gestational diabetes mellitus (GDM) is a pregnancy-related metabolic disease which will influence the health of the mother and the infant, inducing a series of alarming outcomes [1]. An epidemiological study on more than 10,000 pregnant women in 18 cities in China found that the incidence of GDM was 4.3–5.1% [2], and that of other countries or regions was 3–30% [3]. Diagnosis and intervention in the early stage of GDM will improve the life-long health of the two generations; thus, understanding the mechanism of GDM is the first step.

Thioredoxin-interacting protein (TXNIP), also known as vitamin D<sub>3</sub> upregulated protein 1 or thioredoxin-binding protein 2 [4], acts as an oxidative stress-sensitive protein, transfers from the nucleus to the mitochondria, and participates in the redox process of mitochondria [5]. In patients with GDM, the secretion of antiangiogenic factors and proinflammatory cytokines is elevated partly as a result of the occurrence of oxidative stress [6]. Oxidative stress results in the inhibition of migration and infiltration of placental trophoblast cells, causing the placenta to be shallowly implanted [7, 8]. Mitochondria

will be subsequently damaged, and the mitochondria dysfunction affects the development of the placenta and further affects the growth of the fetus [9]. Moreover, most of the redox processes occur in mitochondria; thus, oxidative stress and the accumulation of excessive reactive oxygen species (ROS) make the function of mitochondria even more impaired. The placenta is a highly energy-consuming organ; however, the function of mitochondria in the placenta has not been identified in patients with GDM. TXNIP is highly expressed in renal tubular cells stimulated by increased blood glucose and kidney tissues of diabetic animals and patients with diabetic nephropathy complications [10]; however, in other research, there was no difference of TXNIP DNA methylation between GDM and type 1 diabetes [11]. Although TXNIP also acts as glucose-sensitive protein, its expression state in the placenta of women with GDM and its role in the development of GDM remain unclear. In streptomycin-induced diabetic mice, the increased expression of TXNIP in vascular endothelial cells induces oxidative stress [10], promoting the generation and accumulation of ROS [12], which, in turn, results in mitochondrial apoptosis and is followed by cell apoptosis [13]. Thus, we raised the following hypothesis: in GDM, TXNIP might be highly expressed in the placenta, inducing the accumulation of ROS and oxidative stress, which will compromise the mitochondria, damage the function of the placenta, and influence the health of the mother and infant.

In this study, the expression of TXNIP in the placentas of patients with GDM was explored, and a cellular model was used to elucidate the regulating network of TXNIP; further, the effect of high glucose on the placenta trophoblast cells and the underlying mechanism were studied to verify our hypothesis. At the same time, we proved that high glucose (HG) promotes soaring expression of TXNIP in placental trophoblast cells, leading to accumulation of ROS and the dysfunction of mitochondria. The results will provide the experimental data for the etiological treatment of GDM and further improve the evaluation of placenta function in GDM.

## METHODS

### Immunohistochemistry

The tissue samples evaluated in our study were obtained from 10 puerperae with GDM and 10 healthy puerperae. GDM was diagnosed from the results of 75-g oral glucose tolerance tests (OGTT) at different time points during 24–28 weeks' gestation if at least of the following was true: fasting plasma glucose  $\geq 5.1$  mmol/l and/or 1-h plasma glucose  $\geq 10.0$  mmol/l, and/or 2-h plasma glucose  $\geq 8.5$  mmol/l, respectively. All persons enrolled in the study had no relevant medical history; and patients with GDM managed their blood glucose only via diet. The tissue samples were collected during the delivery process, performed in the Department of Gynecology of the Inner Mongolia People's Hospital between November and December, 2018. The study was approved by the ethics committee of the hospital, and the specimen providers provided informed consent. Information about pregnant women and their newborns is shown in Table 2.

Frozen sections were permeabilized with 0.1% Triton X-100 (cat# T0694, AMRESCO) in PBS (cat# C10010500BT, Gibco, CN). Frozen sections were incubated with 10% goat serum albumin and 1% Triton X-100 at 37 °C. After 0.5 h, sections were incubated with rabbit monoclonal anti-TXNIP (dilution 1:1000, cat# ab215366, Abcam, Cambridge, UK) at 4 °C overnight and then for 1 h with the anti-rabbit Alexa Fluor 488 (cat# A11008, Life Technologies, Grand Island, NY). After 2 h, nuclei were counterstained using 4,6-diamidino-2-phenylindole (DAPI, cat# D9542, Sigma, USA). Stained sections were visualized with an inverted confocal microscope (Leica Microsystems).

### Cell Culture

Human placenta trophoblast cells, HTR-8/SV-neo cells (cat # CRL-3271), were purchased from American Type Culture Collection (ATCC, Rockefeller, MD, USA). HTR-8/SVneo cells were cultured in Roswell Park Memorial Institute 1640 Medium (RPMI1640, cat# 11875-093,

Gibco, USA), containing 5.5 mM glucose, supplemented with 10% (v/v) fetal bovine serum (FBS, cat# 10091-148, Gibco, USA) and 1% (v/v) antibiotics (100 U/mL penicillin and 100 µg/mL streptomycin) (cat# 15140-122, Gibco, USA) at 37 °C in a humidified 5% CO<sub>2</sub> atmosphere.

### HG Treatment

HTR-8/SVneo cells were trypsinized and seeded into 6-well plates (Corning, Acton, MA) at a density of  $2.5 \times 10^5$  cells/well. Cells were cultured in 5.6 mM D-glucose of RPMI 1640 medium for 24 h, then stimulated with various concentrations (0, 2.8, 5.6, 11.2, 25, and 40 mM) of D-glucose for 6 h. Cells were treated with 25 mM L-glucose as an osmotic control. D-Glucose (cat# G7021) and L-glucose (cat# G5500) were purchased from Sigma–Aldrich (St. Louis, MO, USA).

### Transfection Experiment

Human pCMV3-TXNIP (HG16553-UT) and control pCMV3-Negative Control Vector (pCMV3-NCV; CV011) were purchased from Sino Biological (BJ, CN). Cells were seeded into 6-well plates at a density of  $2 \times 10^5$  cells/well. Lipofectamine LTX and Plus reagent (cat# 15338-100, Invitrogen, Van Allen Way Carlsbad, CA) were used according to the manufacturer's protocol for transfection of plasmid DNA into the cells. After seeding for 24 h to approximately 60% confluence, cells were transfected with plasmid DNA at a final concentration of 0.28 µg/mL and cultured in the absence of antibiotic. Transfected cells expressed red fluorescence protein (RFP), which enabled their identification. Cells were further assayed by real-time quantitative PCR (qRT-PCR) and Western blotting at 3 h and 6 h after transfection, respectively.

### Cell Proliferation Assay

HTR-8/SVneo cells were trypsinized and seeded into 96-well plates at a density of  $8 \times 10^3$  cells/well for 24 h. To assess the cell proliferation, the number of cells with red fluorescence was

monitored at 1.5-h intervals for 117 h after transfection with pCMV3-TXNIP or pCMV3-NCV. The high definition automated imaging system of IncuCyte was used in the red fluorescent channel following the manufacturer's instructions (Essen Bioscience, USA).

### Cell Migration Assay

Cell migration was evaluated by a scratch-wound assay using IncuCyte. To examine the HTR-8/SVneo cell migration in the context of enhanced expression of TXNIP, cells were plated into 96-well plates at a density of  $3 \times 10^4$  cells/well. After 12 h of seeding, cells were transfected with pCMV3-TXNIP or pCMV3-NCV and then the transfected cells were grown to confluence for another 12 h. The 96-well wound maker was used to generate a wound in a monolayer of confluent cells and then debris was washed away. Images of cells migrating into the wound space were automatically acquired by the IncuCyte Imaging System at 1-h intervals for 40 h. The data was analyzed using an integrated metric of IncuCyte, and the percentage of red object was counted within the wound.

### RNA Extraction and qRT-PCR Analysis

Total RNA was extracted from HTR-8/SVneo cells using Trizol reagent (cat# 15596018; Life Technologies, USA) according to the manufacturer's instructions. Complementary DNA (cDNA) was prepared using a Prime Script™ RT reagent Kit (cat# RR047A, TaKaRa, CN). qRT-PCR was performed with TB Green™ Premix Ex Taq™ II (cat# RR820A, TaKaRa, CN) using a CFX96 Connect real-time system (Bio Rad, UK). β-actin was used to normalize the data. The primer sequences are described in Table 1. qRT-PCR was performed in triplicate, and the relative expression of genes was calculated using the  $2^{-\Delta\Delta CT}$  method.

### Western Blot Analysis

Cells were harvested at 6 h after HG treatment or transfection. The protein extracts were

**Table 1** Primer sequences of the detected genes

Name	Sequence (5'–3')
β-actin forward	TCCCTGGAGAAGAGCTACGAGC
β-actin reverse	TGCCACAGGACTCCATGCCCG
TXNIP-1 forward	TGCCACCACCGACTTATACTGA
TXNIP-1 reverse	CCTGCTGACCACCTCCTACA
TXNIP-2 forward	GCCAGCCAACTCAAGAGACAA
TXNIP-2 reverse	CAGACACCCGCCCATCAG
TRX forward	GTCAGGATGTTGCTTCAGAGTGT
TRX reverse	CACCCACCTTTTGTCCCTTCTT
Caspase-3 forward	CCTACAGCCCATTCTCCATACG
Caspase-3 reverse	TGCCTCACCACTTTAGAACATTT

prepared with ice-cold lysis buffer RIPA (cat# R0020, Solarbio, BJ, CN) containing protease inhibitor phenylmethylsulfonyl fluoride (PMSF) (cat# P0100, Solarbio, BJ, CN). Protein concentrations of the lysates were measured with the bicinchoninic acid kit (cat# 23227, Pierce, Rockford, IL, USA). Equal amounts of protein extracts (15 μg) were loaded in each lane with loading buffer (cat# P1040, Solarbio, BJ, CN). Samples were boiled for 10 min before being separated on 12% SDS-PAGE gels (cat# 161-0175, Bio-Rad Laboratories, USA), then transferred to polyvinylidene difluoride (PVDF) membranes (Bio-Rad Laboratories, USA), blocked with 5% Difco Skim Milk (cat# 232100, BD, Sparks, MD, USA) and detected using the following primary antibodies: TXNIP antibody (dilution 1:1000, cat# ab215366, Abcam, Cambridge, UK), caspase-3 antibody (dilution 1:1000, cat# 9662, Cell Signaling, Boston, MA), β-actin antibody (dilution 1:1000, cat# G043, Abm, Richmond, BC, CA) at 4 °C overnight, and secondary antibodies: anti-mouse IgG (dilution 1:1000, cat # HAF007, RD, Minneapolis, USA) or anti-rabbit IgG (dilution 1:1000, cat # HAF008, RD, Minneapolis, USA) for 1 h. Detection of β-actin on the same membrane was used as a loading control. Bands were visualized by enhanced chemiluminescence (Bio-Rad Laboratories, USA) with an imaging system (GE Healthcare Life Sciences,

UK) and quantified by Analysis Software Version 1.0 (GE Healthcare Life sciences).

### Immunocytochemistry

HTR-8/SVneo cells were fixed with 4% paraformaldehyde and permeabilized with 0.1% Triton X-100 in PBS. After several washes in PBS, cells were incubated with anti-rabbit TXNIP at 4 °C overnight. Staining was visualized using anti-mouse Alexa Fluor 488 (A21200, Life Technologies, Grand Island, NY). Mitochondria were counterstained using Mito Tracker<sup>TM</sup> Red CMXRos (cat# M7512, Invitrogen, Eugene Oregon). Nuclei were counterstained using DAPI. Stained cells were visualized with the Leica fluorescence microscope.

### Detection of Apoptosis

HTR-8/SVneo cells were trypsinized and seeded into 96-well plates at a density of  $1 \times 10^4$  cells/well for 24 h and transfected with pCMV3-TXNIP or pCMV3-NCV. Caspase-3 was measured with Super View 488 Caspase-3 Assay Kit for Live Cells (cat# S6007, Everbright USA Inc.). The Caspase-3 Assay Kit was used as an indicator for apoptosis cells measured with green fluorescence. Briefly, the working solution was prepared at a concentration of 1 μM according to

the manufacturer's instructions. The treated cells were incubated with working solution at 37 °C for 0.5 h, then observed for 117 h by IncuCyte.

### Measurement of Intracellular ROS Production

Cells were seeded into a 24-well plate at a density of  $1 \times 10^5$  cells/well and cultured for 24 h, then transfected with pCMV3-TXNIP or pCMV3-NCV (0.28  $\mu\text{g}/\text{mL}$ ) for 0.5 h. After transfection, cells were incubated with 1  $\mu\text{M}$  of dihydroethidium (DHE, ROS Fluorescent Probe, cat# D1008, CN) at 37 °C for 0.5 h in the dark. The DHE was used as a cell-permeable indicator for intracellular ROS measurement, the red object count. The intracellular ROS levels were measured by Cytation 5 imaging multi-mode reader (Biotek, USA) at 15-min intervals for 10.5 h to detect the intensity of DHE fluorescence (excitation and emission wavelengths at 488 and 525 nm).

### Determination of Mitochondrial Membrane Potential

Mitochondrial membrane potential was measured in HTR-8/SVneo cells using an immunofluorescence technique from the Mitochondrial Membrane Potential Assay Kit with JC-1 (cat# M8650, Solarbio, CN). Cells were balanced for 0.5 h after transfection with pCMV3-TXNIP or pCMV3-NCV. The JC-1 solution was prepared at a concentration of 200 mM according to the manufacturer's instructions. The cells were incubated with 200 mM of JC-1 at 37 °C for 0.5 h in the dark. Cytation 5 cell imaging multi-mode reader was used to observe the fluorescence intensity at 0.5-h intervals for 11 h.

### Statistical Analysis

Statistical analysis of the experimental data was performed using Graphpad Prism 6.0 (Graph-Pad, USA), and the results were presented as mean  $\pm$  SEM. Significant differences were determined by Tukey's multiple comparisons

test.  $p < 0.05$  indicated that the difference was statistically significant.

### Compliance with Ethics Guidelines

This study was approved by the Ethics Committee of the Inner Mongolia People's Hospital, and informed consent was obtained from patients and their family members before the study. All procedures performed in the study involving human participants were in accordance with the ethical standards of the institutional research committee and with the 1964 Helsinki Declaration and its later amendments or comparable ethical standards.

## RESULTS

### Although Blood Glucose is Well Controlled, Expression of TXNIP in GDM Group is Significantly Higher than in Normal Control Group

**Immunohistochemistry of TXNIP in Placenta**  
Blood glucose was  $11.2 \pm 1.0$  mmol/l at the 1-h OGTT in the GDM group vs  $6.2 \pm 0.7$  mmol/l in the normal group; and  $9.6 \pm 1.7$  mmol/l at the 2-h OGTT in the GDM group vs  $5.9 \pm 0.7$  mmol/l in the normal group. Frozen sections were stained with TXNIP antibody and visualized with an inverted confocal microscope. TXNIP was widely expressed in villous tissue of the placenta; however, compared with the placenta of healthy pregnant women, TXNIP was highly expressed in syncytiotrophoblasts of the placenta in pregnant women with GDM. As is shown in Fig. 1, the white arrows indicated syncytiotrophoblasts, and the fluorescence intensity in the GDM group was statistically higher than that in the normal control group.

### Maternal, Fetal, and Placental Characteristics in Study Population

There were no statistically differences in baseline characteristics and clinical information (Table 2), and no statistically differences in gestational BMI, pregestational overweight,

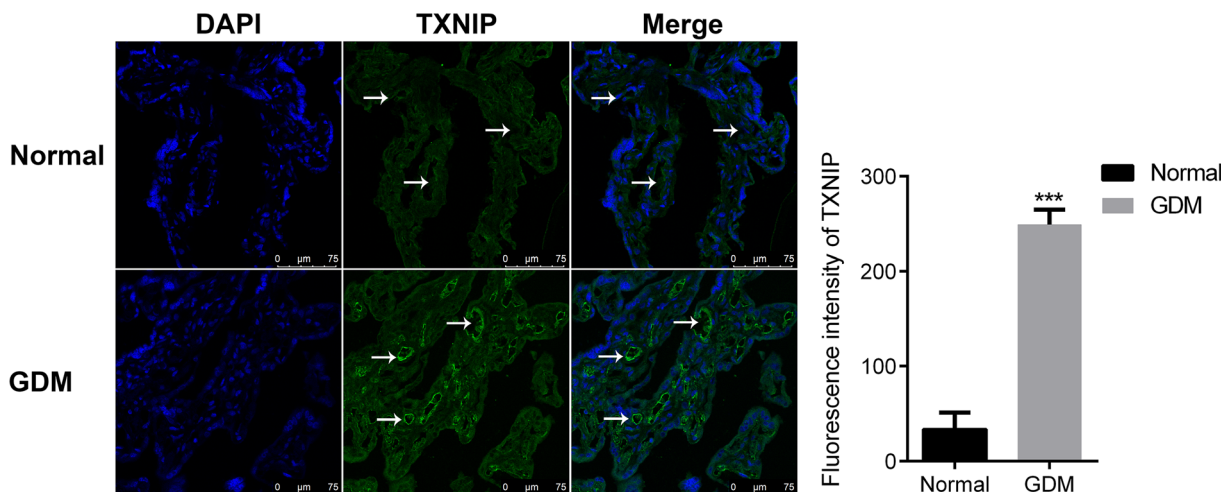


**Fig. 1** Protein expression of TXNIP in the placenta syncytiotrophoblasts of women with GDM was higher than that of the normal group. Frozen placenta sections from the GDM group or normal group were stained with TXNIP antibody. The protein expression of TXNIP in villous tissue of placentas from both groups were investigated via confocal photomicrographs. Green, TXNIP-

positive cells; blue, DAPI for nuclear staining. Scale bar 75  $\mu$ m. Fixed tissue images were captured in a Leica confocal microscope at 40 $\times$ . The white arrows indicate syncytiotrophoblasts, and the fluorescence intensity in the GDM group was higher than that in the normal group, \*\*\* $p < 0.001$  (Tukey’s test) vs normal group

**Table 2** Baseline characteristics and clinical information

Clinical characteristics	GDM ( $n = 10$ )		NOR ( $n = 10$ )		$p$ value
	M	SD	M	SD	
$N$ (total = 20)	10		10		
Height (cm)	163	4.9	163.1	3.6	0.9593
Weight (kg)	74.8	11.8	70.5	9.0	0.3691
Diastolic blood pressure (mmHg)	129.4	8.4	119.8	7.2	0.0535
Systolic pressure (mmHg)	82.1	5.9	72.8	6.7	0.0641
Period of gestation (weeks)	39.0	0.9	39.3	2.3	0.6622
Diagnosis time of GDM (weeks)	24.4	0.7	N/A		
Drug therapy	NO		N/A		

$M$  mean,  $SD$  standard deviation,  $GDM$  gestational diabetes mellitus,  $NOR$  normal,  $N/A$  not applicable

placenta grading, amniotic fluid index (AFI), and fetal weight between patients with GDM and the normal puerperae. However, the blood glucose level based on OGTT in the GDM group is statistically higher than that in the normal control group at three time points. The glucose

level of patients with GDM at three time points was 5.4 (0.8), 11.2 (1.0), and 9.6 (1.7) mmol/l, respectively; the glucose level of the normal group at three time points was 4.3 (0.2), 6.2 (0.7), and 5.9 (0.7) mmol/l, respectively (Table 3).

**Table 3** Clinical characteristics of the subjects and their offspring

Clinical characteristics	GDM ( <i>n</i> = 10)		NOR ( <i>n</i> = 10)		<i>p</i> value
	M	SD	M	SD	
<i>N</i> (total = 20)	10		10		
Age at delivery (years)	29.7	3.8	28.5	2.4	0.4106
Pregestational BMI (kg/m <sup>2</sup> )	28.1	4.0	26.4	2.6	0.3309
Pregestational overweight (BMI ≥ 25 kg/m <sup>2</sup> )	80%		70%		
Fasting plasma glucose (FPG) (mmol/l)	5.4	0.8	4.3	0.2	0.0008
1-h plasma glucose (mmol/l)	11.2	1.0	6.2	0.7	< 0.0001
2-h plasma glucose (mmol/l)	9.6	1.7	5.9	0.7	< 0.0001
HbA1C (%)	6.1	0.3	No		
Placenta grading	II		II		
AFI on the time of first uterine contraction (mm)	132.8	30.3	113.1	27.2	0.1436
Fetal weight (g)	3435.0		3220.0		0.2174

*M* mean, *SD* standard deviation, *GDM* gestational diabetes mellitus, *NOR* normal, *AFI* amniotic fluid index

### High Expression of TXNIP Induced by HG Promoted Morphological Change of Mitochondria and Apoptosis in HTR-8/SVneo Cells

#### Expression of TXNIP Occurred in a Glucose-Dependent Manner

To determine whether mRNA expression of *TXNIP* and *TXN* in HTR-8/SVneo cells was influenced by the concentration of glucose, the cells were treated with 0, 2.8, 5.6, 11.2, 25, and 40 mM of D-glucose, respectively for 3 h; and the expression of *TXNIP* and *TXN* was detected by qRT-PCR. The results showed that the expression of *TXNIP* was gradually raised as the glucose concentration increased from 0 to 25 mM ( $p < 0.001$ ), but it decreased at 40 mM ( $p < 0.001$ ). As is shown in Fig. 2a, the expression level of *TXNIP* is glucose concentration-dependent from 0 to 25 mM. The mRNA expression level of *TXNIP* in 40 mM of glucose is lower than that in 25 mM of glucose ( $p < 0.05$ ), but higher than that in 5.6 mM of glucose ( $p < 0.001$ ). Therefore, 25 mM of glucose was used as HG in the study. On the other hand, the mRNA expression *TXN* remained the

same regardless of the glucose concentration (Fig. 2b). To observe the trend of the protein expression, the proteins of *TXNIP* and *TXN* in HTR-8/SVneo cells cultured in the medium containing 0, 5.6, 25, and 40 mM of glucose for 6 h were detected by western blot. The expression of *TXNIP* protein was the lowest at 0 mM glucose, and over twofold elevation at 25 mM of glucose compared with that at 5.6 mM ( $p < 0.01$ ); the expression of *TXN* protein had no statistically significant change (Fig. 2c, d). The cells treated with 25 mM L-glucose were used as the osmotic control. No expression of *TXNIP* was observed at 25 mM L-glucose; that is to say, the elevated expression of *TXNIP* at 25 mM D-glucose was not caused by osmosis, but the HG (Fig. 2e).

#### Mitochondria Broke into Fragments in HTR-8/SVneo Cells Treated with HG

The morphology of mitochondria in normal glucose (NG, 5.6 mM) and HG (25 mM) was observed. HTR-8/SVneo cells had been cultured in the medium with NG and HG for 6 h, before staining with mitochondrial tracer and *TXNIP* antibody. The morphology of the mitochondria



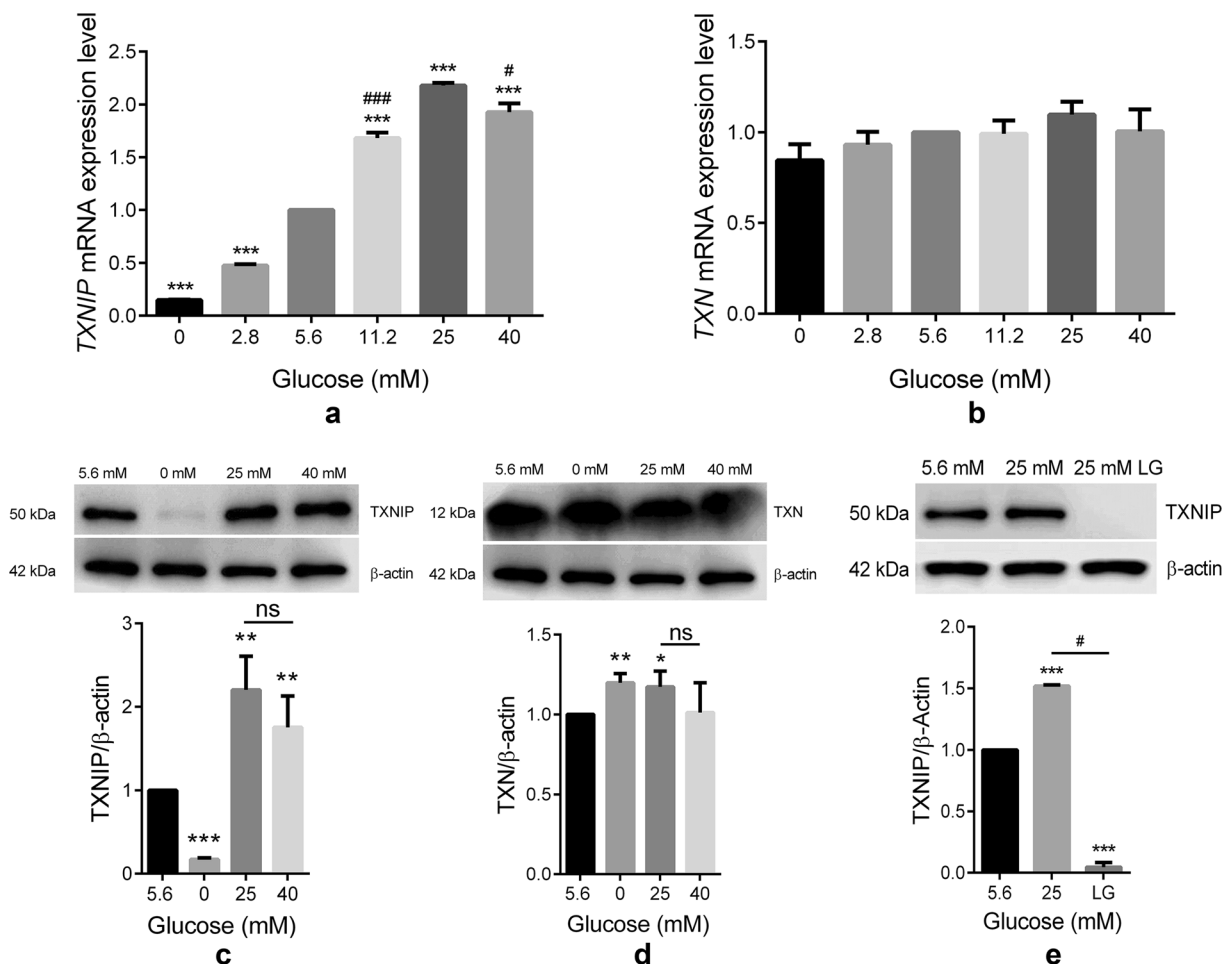


**Fig. 2** TXNIP expression increased in HTR-8/SVneo cells treated with increasing concentration of glucose, but the TXN expression did not. HTR-8/SVneo cells were exposed to the indicated concentration of D-glucose (0, 2.8, 5.6, 11.2, 25, 40 mM) for 3 h. **a** Relationship between mRNA expression of *TXNIP* and the concentration of glucose. The mRNA expression level of *TXNIP* was the highest at the 25 mM of glucose. **b** Relationship between mRNA expression of *TXN* and the concentration of glucose. The mRNA expression level of *TXN* remained statistically the same

although the concentration of glucose changed. **c, d** Respective protein expression of TXNIP and TXN, in the HTR-8/SVneo cells exposed to the indicated concentration of D-glucose (0, 5.6, 25, 40 mM) for 6 h via western blot. **e** HTR-8/SVneo cells were treated with 25 mM L-glucose as an osmotic control and the protein levels of TXNIP were analyzed by western blot. Results were expressed as mean  $\pm$  SEM. \* $p < 0.05$ , \*\* $p < 0.01$ , \*\*\* $p < 0.001$  (Tukey’s test) vs 5.6 mM of glucose. # $p < 0.05$ , ### $p < 0.001$  (Tukey’s test) vs 25 mM of glucose

was observed by confocal microscopy. Consistent with the results found in the western blot, the expression of TXNIP was higher in the HG group than that in the NG group. Obvious changes in the morphology of the mitochondria are shown in Fig. 3. The mitochondria of the NG group were intact and clear while the mitochondrial tubules in the HG group

converted to nodular and many of them formed discrete small mitochondria.

**Cell Apoptosis Was Promoted in HTR-8/SVneo Cells Treated with HG**

To mimic the placental conditions in patients with GDM, HTR-8/SVneo cells were treated with different glucose concentrations (0 mM,

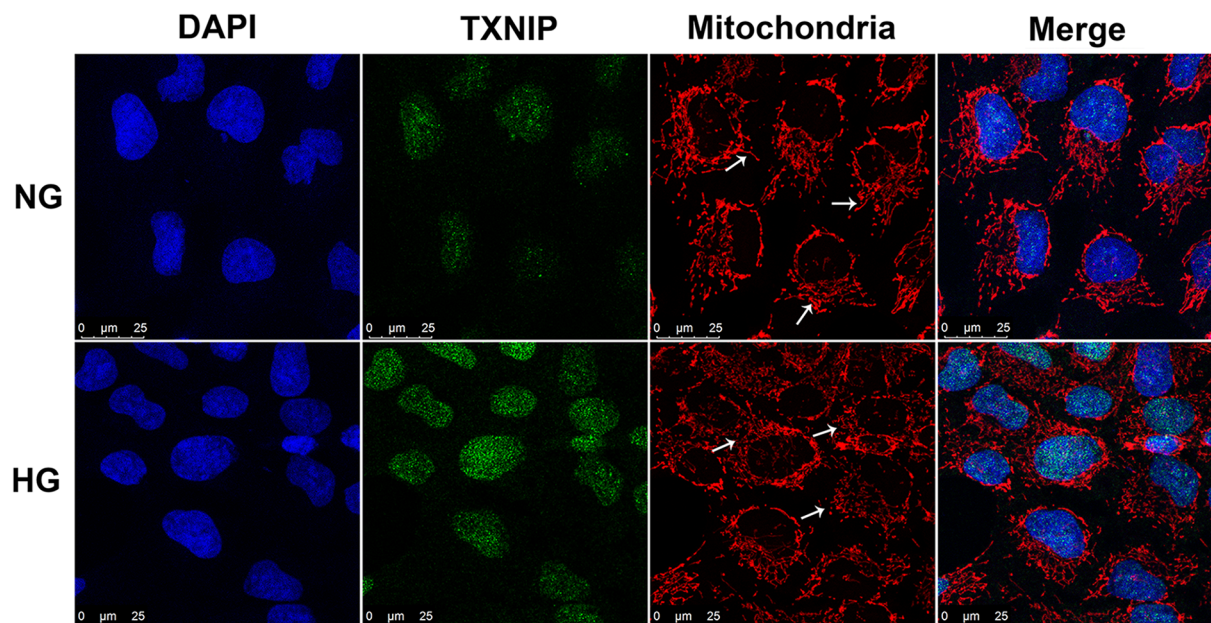


**Fig. 3** Morphological changes of mitochondria caused by high glucose. The white arrows indicate the mitochondria of HTR-8/SVneo cells. The mitochondria broke into nodules or fragments in the HG group, lacking continuity; those in the NG group were intact and clear. NG, HTR-8/

5.6 mM, 25 mM). Caspase-3 is a proteolytic enzyme that mediates cell death and apoptosis. It is the initiator and performer of mammalian apoptosis. After treatment with different glucose concentrations, protein expression of caspase-3 was significantly increased in the 0 mM and 25 mM glucose groups compared with the normal group (5.6 mM) (Fig. 4). Furthermore, the level of caspase-3 in the 25 mM glucose group was statistically higher than that in the 0 mM glucose group, indicating that the apoptosis induced by HG was more exacerbated than that in the situation of starving (0 mM). The level of caspase-3 in the HG-treated group is nearly twofold that in the control group.

#### Overexpression of TXNIP Converted the Phenotype of Cells into Adverse Behavior

##### *Expression of TXNIP and TXN Was Detected After Plasmids Had Been Transfected*

Considering that TXNIP plays an important role in the regulation of oxidative stress and the

SVneo cells cultured in 5.6 mM glucose; HG, cells cultured in 25 mM glucose. Green, TXNIP-positive cells; blue, DAPI for nuclear staining. Scale bar 25 μm. Fixed tissue images were captured in a Leica confocal microscope at 40×

negative relationship between TXNIP and TXN partly governing the balance of the ROS in the cells, the changes of TXN expression level caused by overexpression of TXNIP in HTR-8/SVneo cells was also detected. The cells were divided into the OE-TXNIP group (transfected with the pCMV3-TXNIP), the NC group (transfected with the pCMV3-NCV), and the control group (without transfection). Different from the results reported by other studies which considered the transcriptional changes that occurred at 48 h after transfection [14], the early gene alterations were observed within 6 h after transfection. TXNIP mRNA and protein expression was examined by qRT-PCR and western blotting at 3 h and 6 h after the transfection, respectively. The mRNA expression level of TXNIP in OE-TXNIP group increased 11-fold at 3 h after transfection (Fig. 5a), and the protein expression level of TXNIP increased 30-fold at 6 h after transfection compared with those in the NC group (Fig. 5b); on the contrary, the mRNA expression TXN and its protein (Fig. 5c,

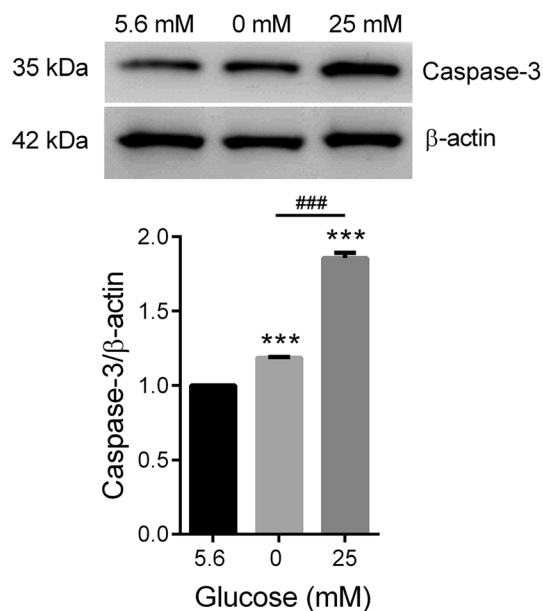


**Fig. 4** Apoptosis was induced by HG in HTR-8/SVneo cells. HTR-8/SVneo cells were cultured in different concentrations of D-glucose (0, 5.6, 25 mM) for 6 h. The data were calculated on the basis of, at least, three independent biological replications; and correspond to mean  $\pm$  SEM. \*\*\* $p < 0.001$  (Tukey's test) vs 5.6 mM of glucose. ### $p < 0.001$  (Tukey's test) vs 0 mM of glucose

d) were correspondingly reduced compared with the NC group.

#### **Overexpression of TXNIP Attenuates Proliferation of HTR-8/SVneo Cells**

The proliferation of HTR-8/SVneo cells with overexpressed TXNIP was investigated via IncuCyte. The transfected cells were labelled with red fluorescent protein. The number of transfected cells was monitored from 12 to 117 h after transfection and counted with an integrated metric of IncuCyte, and the cells with red fluorescence were counted. The inhibition effect on the cells in the OE-TXNIP group became obvious from 48 h after transfection to the end of the observation compared to those in the NC group. A significant decrease in the number of cells with red fluorescence in OE-TXNIP is shown in Fig. 6a. In the NC group, the red fluorescence was diffused evenly in the whole cells; whereas the red fluorescence in the OE-TXNIP cells was gathered in the nucleus,

perfectly reflecting the expression location of TXNIP.

#### **Overexpression of TXNIP Inhibited HTR-8/SVneo Cell Migration**

The migration of HTR-8/SVneo cells overexpressing TXNIP was examined by IncuCyte. As shown in Fig. 6b, the cell migration decreased significantly in the OE-TXNIP cells. Moreover, the inhibitory effect of overexpression of TXNIP on the cell migration began to be evident statistically at 7 h, and the trend continued till the end of observation. At 25 h, significant reduction in wound closure was observed in TXNIP-overexpressing cells.

#### **Cell Apoptosis Was Induced in HTR-8/SVneo Cells Overexpressing TXNIP**

The protein expression level, detected by western blot, of caspase-3 in OE-TXNIP cells was significantly higher than that in the control group and NC group (over 1.5-fold elevation) (Fig. 6d). Meanwhile, the Caspase-3 Assay Kit was used to detect the number of apoptotic cells. Compared with the NC cells, the number of apoptotic cells in the OE-TXNIP group increased in a time-dependent manner and was statistically significant from 24 h on and peaked at 84 h (Fig. 6c).

#### **Underlying Mechanism of Phenotype Change of HTR-8/SVneo Cells Overexpressing TXNIP**

##### **Overexpression of TXNIP Increases ROS Generation**

To investigate ROS generation in the HTR-8/SVneo cells triggered by overexpression of TXNIP, the DHE probe, which is especially sensitive to superoxide ( $O_2^-$ ), was used. By reacting with superoxide ions, DHE forms a red fluorescent product (2-dehydroxyethidium). The curve obtained via the Cytation 5 imaging multi-mode reader displayed a dramatic elevating trend in the first 3 h and also peaked at this time point in the OE-TXNIP group (Fig. 7a). However, ROS accumulation in the NC group only had a slight increase during the first 3 h and peaked at 5 h; similarly, ROS accumulation

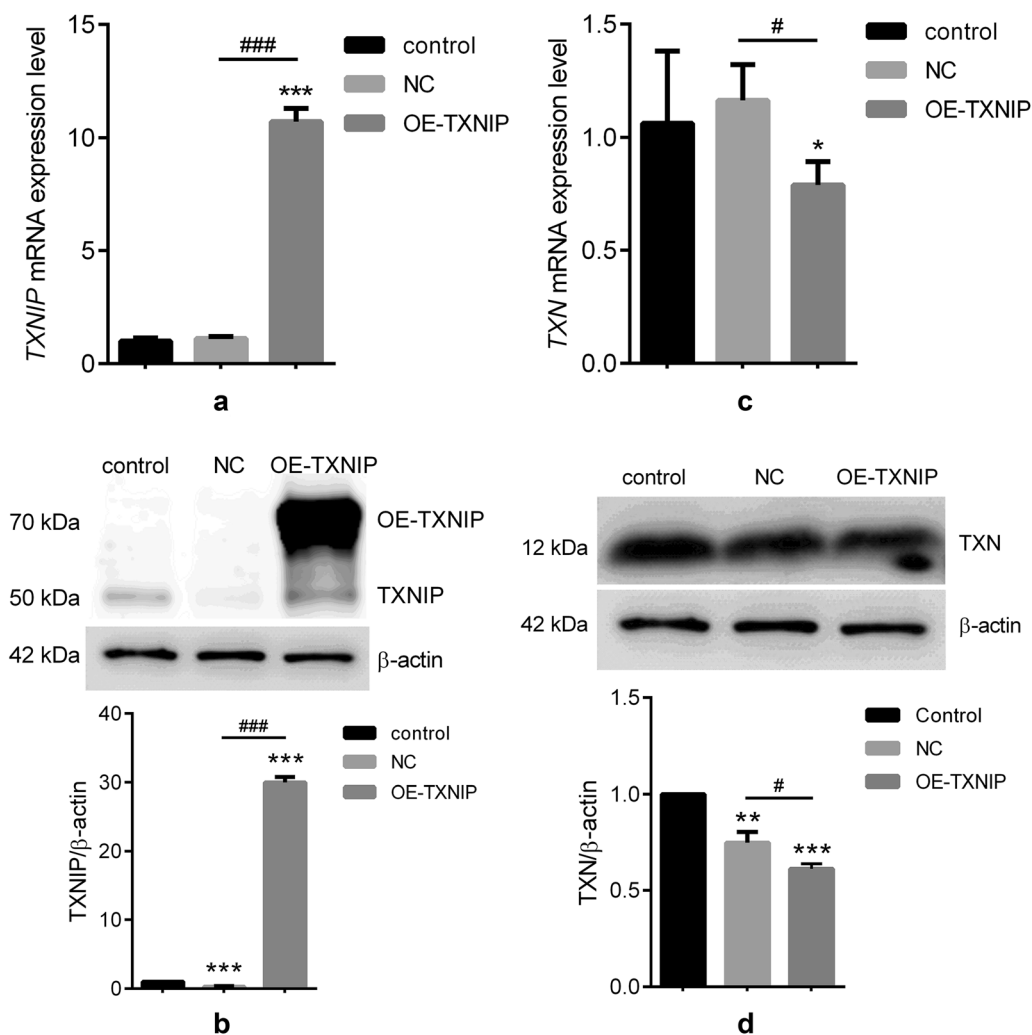


**Fig. 5** TXNIP was overexpressed via plasmid in HTR-8/SVneo cells. HTR-8/SVneo cells were transfected with pCMV3-TXNIP or pCMV3-NCV (0.28  $\mu$ g/mL) for 3 h. The mRNA expression of *TXNIP* and *TXN* was analyzed. **a** Comparison of the mRNA expression of *TXNIP* in the control group, normal control group (NC), and OE-TXNIP group. **b** Protein expression level of TXNIP in different groups. **c** Comparison of the *TXN* mRNA

expression in the control group, NC group, and OE-TXNIP group. **d** Protein expression level of TXN in different groups. The data were analysis based on three independent biological replications and correspond to mean  $\pm$  SEM. \* $p$  < 0.05, \*\* $p$  < 0.01, \*\*\* $p$  < 0.001 (Tukey's test) vs control group (without transfection). # $p$  < 0.05, ### $p$  < 0.001 (Tukey's test) vs NC group (transfected with pCMV3-NCV)

in the control group peaked at 6 h. The fluorescence intensity of cells overexpressing TXNIP was stronger than that in the other two groups (Fig. 7b). Therefore, ROS accumulation was correlated positively with TXNIP expression level in OE-TXNIP (Fig. 7c).

#### **Overexpression of TXNIP Induces Mitochondrial Fragmentation and Mitochondrial Dysfunction in HTR-8/SVneo Cells**

In order to detect whether overexpression of TXNIP causes changes in mitochondrial morphology, cells were transfected for 6 h and then stained with mitochondrial tracer and TXNIP antibody. The mitochondrial morphology was

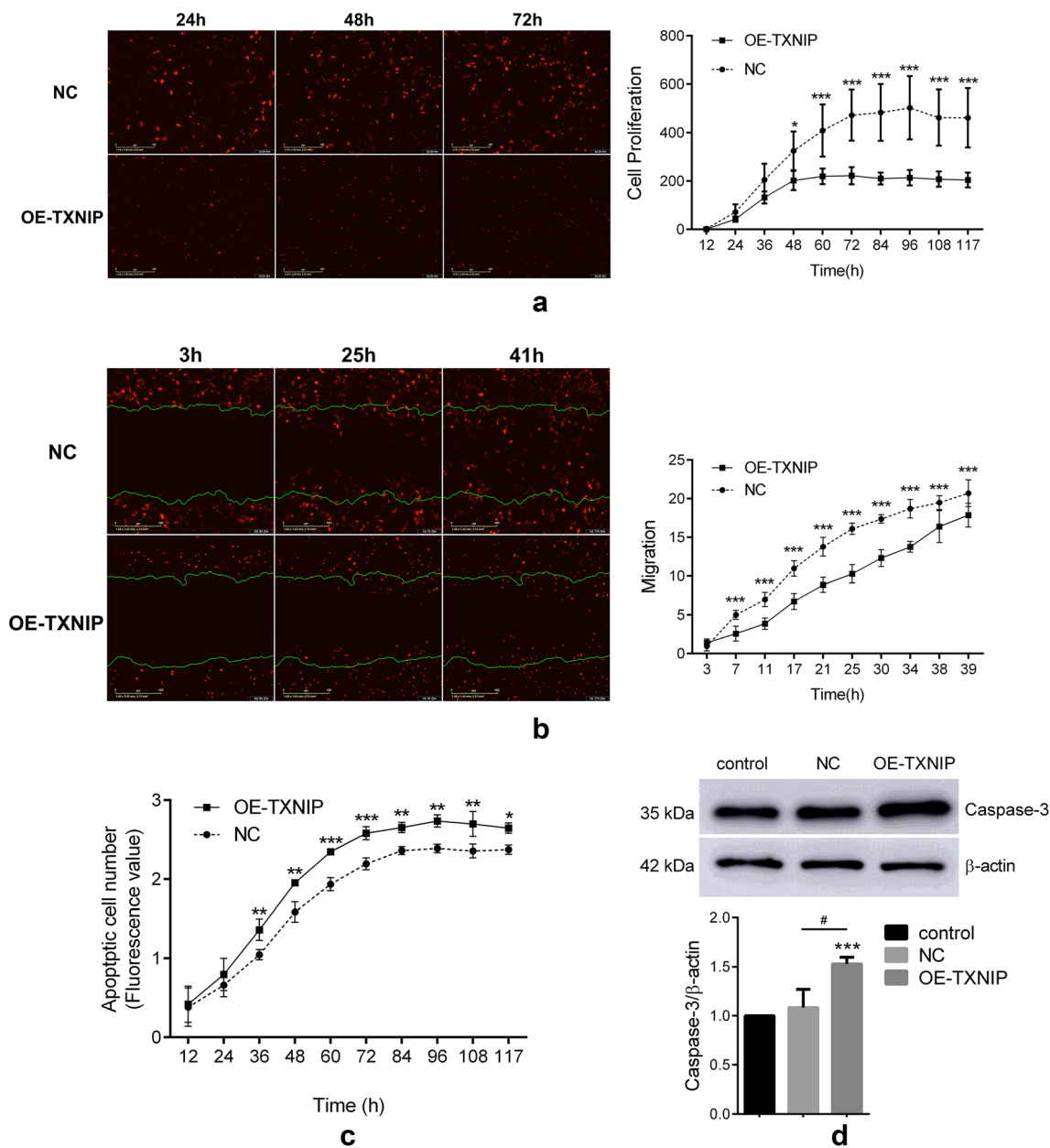


**Fig. 6** Overexpression of TXNIP reduces cell proliferation, inhibits migration, and induces cell apoptosis in HTR-8/SVneo cells. HTR-8/SVneo cells were cultured into 96-well plates then transfected with pCMV3-TXNIP or pCMV3-NCV (0.28 μg/mL). The number of cells with red fluorescence was monitored using the high definition automated imaging system from IncuCyte (Essen BioScience). Images were captured in IncuCyte at ×10. **a** Overexpression of TXNIP inhibited the proliferation of the cells. **b** Cell migration was attenuated in the normal

control group. **c** Apoptosis was severer in the OE-TXNIP group. **d** Caspase-3 protein level was explored by western blot. β-actin was used as control. Control: cells without transfection. The experiments were replicated independently at least three times. Results were expressed as mean ± SEM. \*\*\**p* < 0.001 (Tukey’s test) vs NC group (transfected with pCMV3-NCV). #*p* < 0.05 (Tukey’s test) vs control group. NC normal control group, OE-TXNIP overexpression of TXNIP group

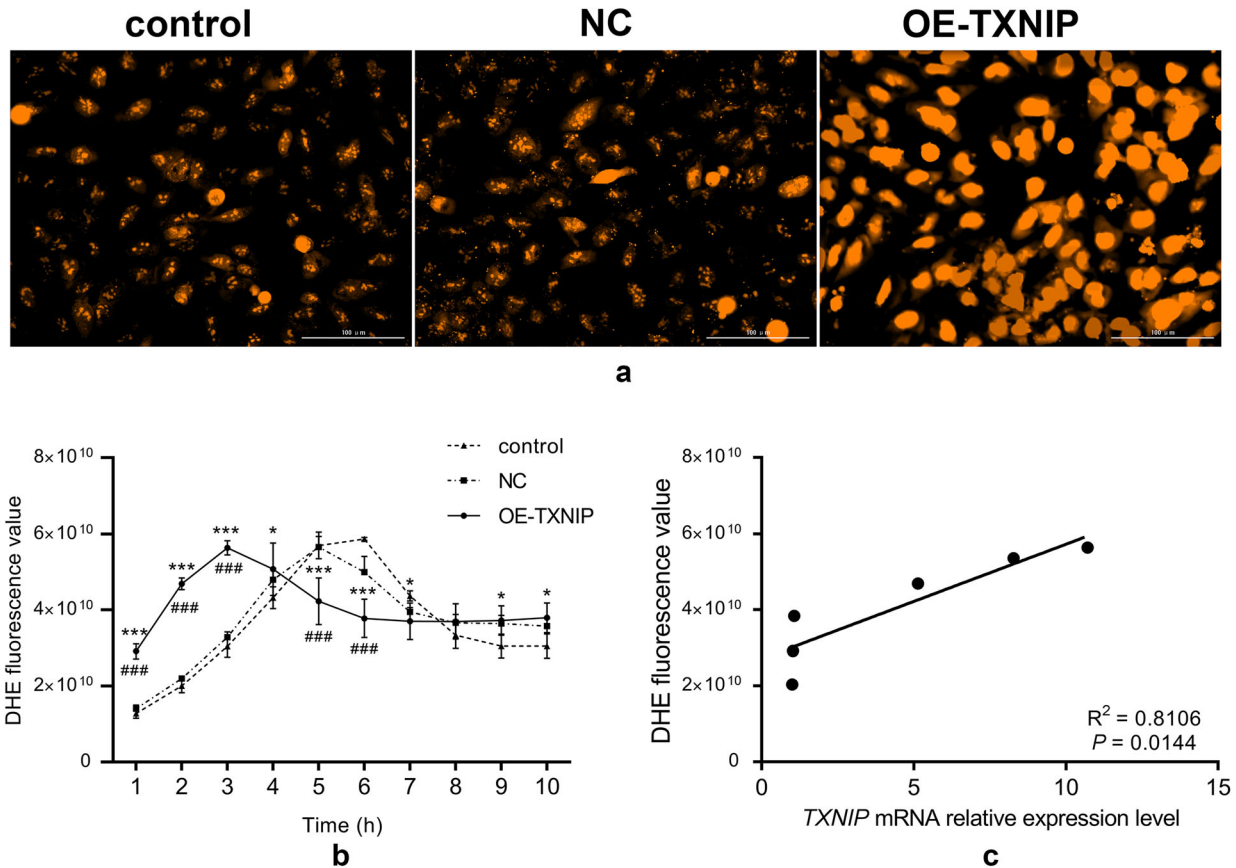


**Fig. 7** Overexpression of TXNIP increases ROS generation in HTR-8/SVneo cells. HTR-8/SVneo Cells were transfected with pCMV3-TXNIP or pCMV3-NCV (0.28  $\mu\text{g}/\text{mL}$ ). ROS generation marked by 1  $\mu\text{M}$  DHE fluorescence. **a** Overexpression of TXNIP led to the accumulation of ROS. The fluorescence intensity reflected the accumulated level of ROS. The accumulation of ROS climbed to the peak at 3 h after TXNIP was transfected. Images were captured in Biotek at  $\times 20$ . **b** Number of cells with red fluorescence was analyzed using the high

definition automated imaging system from Cytation 5 (Biotek). Control, cells without transfection; NC, normal control group; OE-TXNIP, overexpression of TXNIP group. **c** Analysis of the correlation between TXNIP expression and ROS accumulation. The experiments were replicated independently for at least three times. Results were expressed as mean  $\pm$  SEM.  $###p < 0.001$  (Tukey's test) vs NC group (transfected with the pCMV3-NCV).  $*p < 0.05$ ,  $***p < 0.001$  vs control group

observed via confocal microscopy. It showed that the fluorescence intensity of TXNIP in the OE-TXNIP group was significantly higher than that in the control and NC groups. Significant changes were found in mitochondrial morphology. The mitochondria of the control and NC groups were intact and clear. The mitochondrial tubules in the OE-TXNIP group were nodular, and many of them formed discrete small mitochondria (Fig. 8a). These results indicated that overexpression of TXNIP induced

mitochondrial fragmentation in the HTR-8/SVneo cells.

Cell mitochondrial membrane potential ( $\Delta\Psi$ ) of cells overexpressing TXNIP was analyzed by JC-1 staining. The change of  $\Delta\Psi$  is an important indicator of activation of cell apoptosis [15, 16]. An increase in green fluorescence (JC-1 monomer) is associated with mitochondrial membrane depolarization, whereas an increase in red fluorescence (JC-1 aggregate) is related to polarization of the mitochondrial

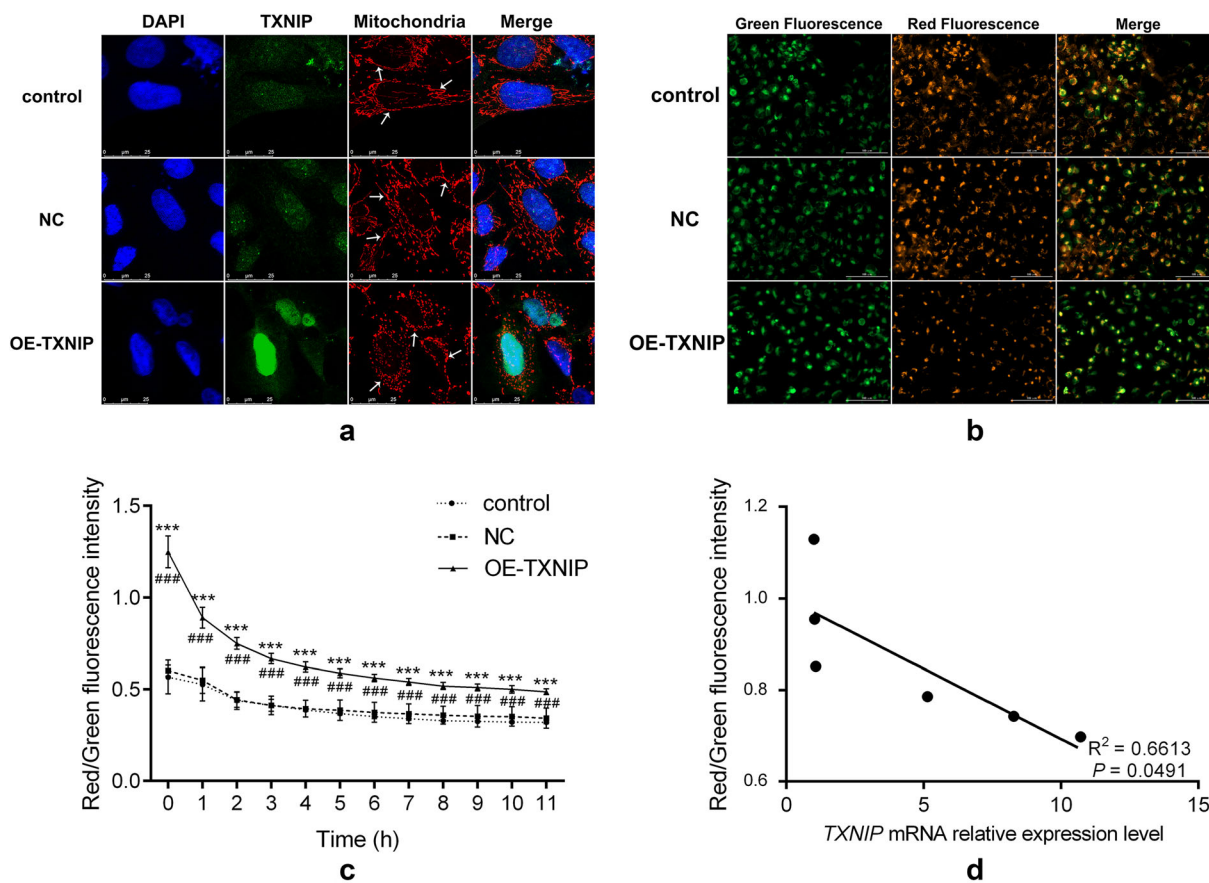


**Fig. 8** Overexpression of TXNIP induces mitochondrial dysfunction in HTR-8/SVneo cells. HTR-8/SVneo cells were transfected with pCMV3-TXNIP or pCMV3-NCV (0.28  $\mu$ g/mL). Mitochondrial morphology was assessed at 6 h after TXNIP was transfected. **a** Overexpression of TXNIP changed the mitochondria of the cells morphologically. The white arrows indicate mitochondria of HTR-8/SVneo cells. The mitochondrial fragmentation observed in the OE-TXNIP group was higher than that in the NC and the control group. Green, cells expressing TXNIP; red, Mito Tracker; blue, DAPI for nuclear staining. Scale bar 25  $\mu$ m. Fixed cell images were captured in a Leica confocal microscope at  $\times 40$ . **b** Mitochondrial membrane potential decreased in the OE-TXNIP group. The mitochondrial membrane potential marked by 200 mM JC-1. Overexpression of TXNIP decreased the

mitochondrial membrane potential to the lowest point at 3 h after TXNIP was transfected. Red fluorescence represents cells with intact mitochondrial membranes, and green fluorescence represents the cells with loss of mitochondrial membrane potential. Images were captured in Biotek at  $\times 20$ . **c** The ratio of red fluorescence intensity to green fluorescence intensity was analyzed to quantify the mitochondrial membrane potential ( $\Delta\Psi$ ) of the cells. **d** Analysis of the correlation between TXNIP expression and mitochondrial membrane potential ( $\Delta\Psi$ ). The experiments were replicated independently at least three times. Results were expressed as mean  $\pm$  SEM. ### $p < 0.001$  (Tukey’s test) vs NC group (transfected with pCMV3-NCV). \*\*\* $p < 0.001$  vs control group (without transfection)

membrane [17]. The loss or reduction of membrane potential in the control, NC, and OE-TXNIP group was monitored at 0.5-h intervals for 11 h. The results showed that mitochondrial potential decreased in a time-dependent

manner (Fig. 8b). JC-1 staining data showed that the OE-TXNIP group exhibited a decline in red fluorescence and an enhancement of green fluorescence compared with that in the control and NC groups (Fig. 8c).  $\Delta\Psi$  was correlated

negatively with TXNIP expression level in the OE-TXNIP group (Fig. 8d). A change from red to green fluorescence in the OE-TXNIP group indicated that overexpression of TXNIP could result in the integrity loss of the mitochondrial membrane in the HTR-8/SVneo cells, which led to severe mitochondrial damage. Thus, it was concluded that TXNIP overexpression induced mitochondrial dysfunction in HTR-8/SVneo cells.

## DISCUSSION

GDM is not only closely related to maternal health but also affects the health of the offspring [18, 19]. GDM and its complications can be alleviated after delivery of the placenta, so the placenta is considered to play a vital role in the pathogenesis of GDM [20]. High calorie intake and unhealthy diet structure are currently widespread, and GDM has become a common social health problem. Excessive calorie ingestion during pregnancy can impede the normal function of trophoblastic epithelium of the placental villous tree and seriously interfere with the formation of the placenta [21]. Glucose transporter 1 (GLUT1) is the main carrier of glucose in the placenta. Within the physiological concentration range of blood glucose, GLUT1 increases with the increase of glucose concentration, but when the blood glucose concentration reaches a certain value, the GLUT1 transporter saturates, which leads to the transfer of glucose to the fetus through placental trophoblast cells [22, 23]. Glucose transporters in the placenta are mainly induced by hyperglycemia in the first trimester of pregnancy [24]. Glucose control during the first trimester of pregnancy has a great impact on placental development and function, especially on uptake, transfer, and utilization of glucose [22]. Changes in glucose transport and transfer during early pregnancy affect embryo implantation and development, and also increase the risk of cardiovascular and metabolic diseases in the adulthood of the fetus [25, 26]. Some studies have found that although patients with GDM have their glucose level strictly controlled within normal range during pregnancy, *GLUT1*

gene expression in placental syncytiotrophoblast cells is twice as high as normal, and glucose transport is upregulated by 40% [27]. In our study, although the blood glucose of patients with GDM had been strictly monitored and controlled, which was reflected by the average value of HbA1c ( $6.1 \pm 0.3$ ), the expression of TXNIP in the placenta displayed by immunofluorescence is higher than that in normal puerperae. This phenomenon highlights that it is important to precisely make the treatment based on the expression level of TXNIP besides blood glucose management. Hyperglycemia during GDM can lead to changes in placental function. Therefore, in the metabolism of glucose in the placentas of patients with GDM, the toxicity from HG to the placenta should be taken into consideration besides glycemic transfer [28].

At present, the main biochemical test for GDM is OGTT, which is used for the diagnosis and classification of GDM, but not for the risk assessment of perinatal adverse outcomes [29]. The clinical prediction of perinatal outcomes is mainly through Doppler ultrasound or placental weight and birth weight ratio [30]. GDM is undoubtedly caused by multiple factors. Single glycosylated hemoglobin or OGTT determination is unlikely to provide predictive ability of placental development and function. The results from our study for the first time proved the change in expression of TXNIP in the placentas of patients with GDM; and explored the relation between TXNIP and oxidative stress in the placental trophoblast cell line. If one can combine biochemical indicators, which might be drawn from further research of the parallel indicators of TXNIP in the blood, with placenta-specific secretion of oxidative stress protein, it will be the ideal predictor of placental development or perinatal outcomes. That will not only evaluate the prognosis of the offspring but also help early prediction, prevention, and intervention in GDM.

A clinical follow-up study of placenta and offspring of 38 pregnant women with preeclampsia (preE) found that the placenta was oval in shape rather than round, and the offspring had a higher risk of hypertension [31]. In our study, no significant difference in placental



morphology was found between the GDM group and the healthy puerperae (control group); furthermore, the weights of the fetuses were positively correlated with the values of OGTT of the corresponding mothers, which is consistent with the results from another study [32].

Studies on the molecular mechanism of glucose toxicity in the placenta are still unclear. Some researchers regarded ROS as a mediator which plays an important role in this process [33, 34]. Abnormal expression of TXNIP has been defined as the initiation of a series of reactions to oxidative stress, mitochondrial damage and apoptosis, and in most tissues tested, including pancreatic and retinal cells, the expression of TXNIP is induced by HG under diabetes mellitus pathological circumstances [35–38]. TXNIP is mainly located in the cytoplasm and nucleus. During cellular stress, TXNIP translocates into mitochondria, induces oxidative stress, and leads to the morphological change of mitochondria which provide energy for normal placental development [39], and it is still unclear about its metabolic signal transduction mechanisms in placenta. Mitochondrial dysfunction or abnormal energy supply will directly lead to abnormal placental function and dysplasia, cause perinatal complications, and affect fetal growth and development [25, 40]. As we all know, the placenta is an organ that provides nutrients and energy to the fetus. Studies have found that mitochondrial enzyme activity in skeletal muscle of pregnant women with GDM was reduced compared with normal pregnant women [41], and the expression levels of *AMPK*, a gene in placenta closely associated with mitochondrial phosphorylation and ATP production, were significantly elevated [42], and the mitochondrial morphology of syncytiotrophoblast cells was abnormal [43], strongly indicating that mitochondrial function might be impaired. Recently, Holland et al.'s review of gestational complications considered that changes of mitochondrial number were not consistent and may increase or decrease in the same pathological course; the duration of the damage to the tissue may be the cause for it [44]. In some diseases, mitochondrial changes are considered as a compensatory mechanism

for cell damage [45–47]. On the other hand, ROS produced in mitochondria can damage mitochondrial DNA (mtDNA) and cell membranes, thus inhibiting mitochondrial adaptive stress ability. Therefore, considering the dysfunction of the placenta in patients with GDM from the perspective of mitochondrial content, structure and function and oxidative stress may become a new perspective for evaluating perinatal outcomes.

This study discussed the role of TXNIP in the placentas of patients with GDM. First, we excluded factors that might affect placental function, such as smoking, drinking, and pathological diseases of the mother or fetus. Secondly, in order to avoid affecting the placental metabolism during delivery, we selected full-term placentas in cesarean section. Placental tissues of 10 patients with GDM (GDM group) and 10 normal pregnant women (control group) were collected. Immunofluorescence detection of placental tissue sections showed that TXNIP was highly expressed in the syncytiotrophoblasts of placentas in the GDM group compared with that in the control group. The expression of *TXNIP* gene in placental trophoblast cells was positively related to the fetal weight, indicating that TXNIP was involved in the GDM pathogenesis and fetal development. At present, there are few studies on GDM placental development, and the existing data cannot provide consistent conclusions. Kinalski et al. reported that lipid peroxidation was increased in placentas of women with GDM, but superoxide dismutase (SOD) activity was decreased compared with the control group [37]. In contrast, Pustovrh et al. failed to find any difference in placental lipid peroxidation or SOD between normal pregnant women and pregnant women with GDM [48]. In recent studies, it has been observed that serum malondialdehyde (MDA) level in patients with GDM is higher than that in normal pregnant women, and SOD is lower than that in healthy pregnant women. MDA, as the final product of lipid peroxidation mediated by ROS, indicates the oxidative status of the blood. These data suggest that oxidative stress and its related molecules play an important role in GDM. However, in the study, limited sample size

hindered the capacity to assess the impact of TXNIP on placentas of women with GDM.

To further clarify the role of TXNIP in placental dysfunction and adverse pregnancy outcomes, in this study we used HTR-8 cells of placental trophoblasts for in vitro experiments and found similar results after treatment with different concentrations of D-glucose. Significant high expression of TXNIP transcription and protein levels were observed when placental trophoblast cells were stimulated with high concentrations of D-glucose (25 mM) for 3 h. Similarly, TXNIP is highly expressed in the kidneys of patients with type 2 diabetes mellitus (T2DM), in mice kidneys induced by streptozotocin, and renal tubular cells stimulated by HG [12, 49]. Studies have shown that the high expression of TXNIP induced by D-glucose can cause positive self-feedback [50]. Therefore, in our research, the expression of TXNIP was 15 times higher than that of the normal control when stimulated with D-glucose. A possibility might be that the excessive glucose bind to ChoRE, the promoter region of *TXNIP* gene, induces the expression of TXNIP, followed by expression amplification because of the positive self-feedback [51]. The high expression of TXNIP in type 2 diabetic nephropathy is considered to promote the generation and accumulation of ROS [12]. In this study, DHE fluorescent probe was used for real-time measurement through the BioTek live cell workstation. It was found that the overexpression of TXNIP promoted the activity of ROS in HTR-8 cells in a time-dependent manner and peaked at 3 h. This indicates that the expression of TXNIP is positively correlated with the accumulation of ROS, which indicates that TXNIP promotes oxidative stress, which is consistent with previous studies. The limitations of DHE include the instability of the probe and its products [52]. We can eliminate the disadvantages by specific excitation wave separation and real-time detection, and hence can better reflect the real state of cells [53]. Placental syncytiotrophoblast cells are particularly sensitive to ROS, especially in early pregnancy [54], and the damage to the placental trophoblast cells by ROS is irreversible. In a recent review, gestational complications such as intrauterine growth retardation

(IUGR), spontaneous preterm birth, early eclampsia, oxidative stress prevalent in the placentas of patients with GDM [55], and perinatal outcomes are closely associated with oxidative stress.

The accumulation of ROS induces mitochondrial apoptosis and apoptosis of the cell [56]. Previous studies also found oxidative stress, mitochondrial dysfunction, and endoplasmic reticulum stress in peripheral tissues of patients with GDM [41, 57]. Studies on glucotoxicity in T2DM have found that the high expression of TXNIP leads to the accumulation of ROS, which accelerates islet  $\beta$ -cell apoptosis [50]. We detected caspase-3 in HTR-8 cells by western blot in the exogenous TXNIP-overexpressing cells and found that the expression of caspase-3 protein was increased significantly, and, real-time detection of caspase-3 fluorescence showed that the caspase-3 fluorescence value of TXNIP-overexpressing cells was stronger than that of control group cells over time, proving that HTR-8 cells entered the apoptosis stage induced by the accumulation of ROS which was led by the overexpression of TXNIP. In their real state, the syncytiotrophoblast cells cannot reproduce on their own [58]; thus, their apoptosis will leave incomplete loopholes on the placenta [59], which will damage the protecting barrier role of the placenta. As was shown in preE and IUGR, the apoptotic cells cause gaps on the trophoblast [60]. The fibrin gathering and depositing in the gaps that are recognized as placenta villus detachment, through which excess concentrations of glucose or other harmful ions invade into the blood circulation of the fetus, influence the regulation of the gene expression of the fetus [59, 61]. In present study, the proliferation and migration of HTR-8/SVneo cells were inhibited in the TXNIP overexpression group; the overexpression of TXNIP leading to excessive damage of mitochondria and the accumulation of ROS might be the reason, which is similar to the pathogenesis of most neurodegenerative diseases and diabetic retinal diseases [62, 63]. Studies have shown that IUGR and abnormal proliferation, migration, and invasion of placental trophoblast cells in the pathogenesis of

preE of pregnancy are the key factors inducing the onset of the disease [64, 65].

HG induces the expression of TXNIP in cells and interacts with thioredoxin (TXN) to form TXN/TXNIP redox-related protein complexes called redox enzymes, which weaken the antioxidant activity in the intracellular environment, increase free diffusion of hydrogen peroxide ( $H_2O_2$ ), inhibit the antioxidant activity of TXN [10], cause oxidative stress, and participate in the pathogenesis of many diseases, including autoimmune diseases and degenerative diseases [66]. Silencing the *TXNIP* gene in HG induces less production of ROS by human aortic endothelial cells than wild-type cells and supports the inhibitory effect of TXNIP on TXN redox activity [67]. Studies proved that the expression of TXN decreased as TXNIP increased. In this study, the expression of TXNIP increased with the D-glucose concentration, but no inhibition of expression of TXN was found. However, when TXNIP was overexpressed by plasmid transfection up to 15 times as high as that in the normal control cells, the expression of TXN began to decrease 6 h after the transfection. The underlying mechanism might be as follows: First, the balancing threshold of the TXN/TXNIP complex is different according to different tissues. The change in expression of TXNIP caused by D-glucose was not enough to trigger the change of TXN, but when the expression of TXNIP was up to 30-fold, the change of TXN was observed. Second, the placenta is a temporary organ during a certain period, and it bridges the metabolism of the mother and fetus; thus, buffering is the main function besides its strong endocrinological role. When the acute change of the gene expression happens, the placenta conducts the buffering job to weaken the change, offset the change of TXNIP caused by the glucose, but when the expression level of TXNIP is beyond the buffering ability, the placenta does not do the job, resulting in changes of TXN and TXNIP, inducing ROS accumulation in a short time.

At present, it is unclear how mitochondrial dysfunction, ROS, and TXNIP are related in the mechanism of placental development in GDM. Current studies indicate that TXNIP may be located upstream of the two processes

mentioned above. The expression of TXNIP is induced by glucose, and the increase of TXNIP can stimulate the generation of ROS [10]. Our study found that the increasing expression of TXNIP is positively correlated with the accumulation of ROS. Therefore, TXNIP may be an intermediate connecting the development of GDM and the generation of ROS. We also found that the expression of TXNIP was positively correlated with mitochondrial membrane potential change (JC-1). Compared with the normal control group, the overexpression of TXNIP led to translocation from the nucleus to the mitochondria, turning the mitochondria into nodules. Mitochondrial function is dependent on mitochondrial structure, which in turn is dependent on mitochondrial dynamics, including division, fusion, and movement [68]. Recent studies found that abnormal mitochondrial fusion of cardiac cells in infants born from diabetic or obese mothers increases the risk of heart disease at birth and throughout life [69]. Regarding GDM, the effect of mitochondrial dysfunction caused by the change of TXNIP on the offspring needs further research.

## CONCLUSIONS

This study reveals the molecular mechanism of placental damage in GDM, which can also be applied to the prediction of perinatal outcomes (Fig. 9). The expression of TXNIP increased significantly in the placentas of patients with GDM. When TXNIP was highly expressed in HTR-8 cells stimulated by HG, the mitochondrial function was decreased, the accumulation of ROS and an increase of apoptosis were observed, and the proliferation and migration ability of the cells was impeded. Therefore, TXNIP plays an important role in the metabolism of the placenta in patients with GDM and participates in GDM placental dysfunction via increasing ROS and mitochondria dysfunction. The results will provide the basis for new methods of detecting placental function and for future interventions.

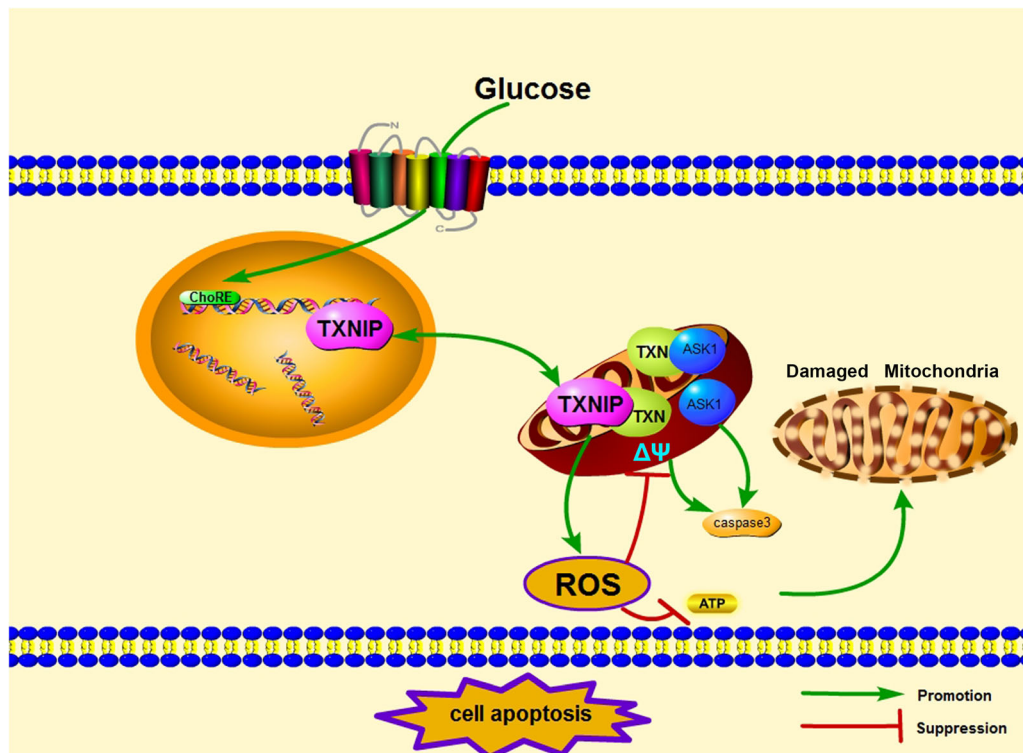


**Fig. 9** Model of the cell apoptosis procedure that happens in the HTR-8/SVneo cells with high expression of TXNIP treated with HG. TXNIP expression is strongly induced in HTR-8/SVneo cells treated with HG. TXNIP is primarily located in the cytoplasm and nucleus. TXNIP translocates into mitochondria where it interacts with TXN when cellular stress occurs. The combination of TXNIP with

TXN attenuates the reducing ability of TXN, increases ROS accumulation, and results in mitochondrial dysfunction (morphological change and inhibition of ATP generation). TXNIP can also release ASK1 from the TXN–ASK1 complex. The released ASK1 turns on the pathway of apoptosis, which leads to cleavage of caspase-3 and cell apoptosis

## ACKNOWLEDGEMENTS

The authors thank all participants for their cooperation and sample contribution.

**Funding.** This research and the journal's Rapid Service Fee were supported by the Natural Science Foundation of Inner Mongolia (Grant No. 2016BS0315) and the National Natural Science Foundation of China (Grant No. 81860277). All authors had full access to all of the data in this study and take complete responsibility for the integrity of the data and accuracy of the data analysis.

**Authorship.** All named authors meet the International Committee of Medical Journal Editors (ICMJE) criteria for authorship for this

article, take responsibility for the integrity of the work as a whole, and have given their approval for this version to be published.

**Authorship Contributions.** Conceptualization, L.Y. and Sarina; methodology, Sarina, D.F.L., Z.Q.F., N.H., and Y.Y.W.; software, J.C.J. and Alamusi; validation, L.Y. and Sarina; formal analysis, Sarina; investigation, J.D., W.H.Z., and X.L.J.; data curation, Sarina, Z.Q.F., and D.F.L.; writing—original draft preparation, Sarina, D.F.L., Z.Q.F., and Z.Y.W.; writing—review and editing, L.Y., Sarina, D.F.L., Z.Q.F. and Z.Y.W.; visualization, J.C.J. and Alamusi; supervision, L.Y. and Sarina; project administration, L.Y.

**Disclosures.** Sarina, Dong Fang Li, Zong Qi Feng, Jie Du, Wen Hua Zhao, Na Huang, Jian

Chao Jia, Zhou Ying Wu, Alamusi, Yong Yun Wang, Xiao li Ji, and Lan Yu have nothing to disclose.

**Compliance with Ethics Guidelines.** This study was approved by the Ethics Committee of the Inner Mongolia People's Hospital, and informed consent was obtained from patients and their family members before the study. All procedures performed in the study involving human participants were in accordance with the ethical standards of the institutional research committee and with the 1964 Helsinki Declaration and its later amendments or comparable ethical standards.

**Data Availability.** The datasets generated during and/or analyzed during the current study are available from the corresponding author on reasonable request.

**Open Access.** This article is distributed under the terms of the Creative Commons Attribution-NonCommercial 4.0 International License (<http://creativecommons.org/licenses/by-nc/4.0/>), which permits any noncommercial use, distribution, and reproduction in any medium, provided you give appropriate credit to the original author(s) and the source, provide a link to the Creative Commons license, and indicate if changes were made.

## REFERENCES

- Kim C, Newton KM, Knopp RH. Gestational diabetes and the incidence of type 2 diabetes: a systematic review. *Diabetes Care*. 2002;25:1862–8.
- The HAPO Study Cooperative Research Group, Metzger BE, Lowe LP, et al. Hyperglycemia and adverse pregnancy outcomes. *N Engl J Med*. 2008;358:1991–2002.
- Yang X, Hsu-Hage B, Zhang H, Zhang C, Zhang Y, Zhang C. Women with impaired glucose tolerance during pregnancy have significantly poor pregnancy outcomes. *Diabetes Care*. 2002;25:1619–24.
- Schulze PC, De Keulenaer GW, Yoshioka J, Kassik KA, Lee RT. Vitamin D3-upregulated protein-1 (VDUP-1) regulates redox-dependent vascular smooth muscle cell proliferation through interaction with thioredoxin. *Circ Res*. 2002;91:689–95.
- Saxena G, Chen J, Shalev A. Intracellular shuttling and mitochondrial function of thioredoxin-interacting protein. *J Biol Chem*. 2010;285:3997–4005.
- Burton GJ, Yung HW, Murray AJ. Mitochondrial—endoplasmic reticulum interactions in the trophoblast: stress and senescence. *Placenta*. 2017;52:146–55.
- Han CS, Herrin MA, Pitruzzello MC, et al. Glucose and metformin modulate human first trimester trophoblast function: a model and potential therapy for diabetes-associated uteroplacental insufficiency. *Am J Reprod Immunol*. 2015;73:362–71.
- Cawyer CR, Horvat D, Leonard D, et al. Hyperglycemia impairs cytotrophoblast function via stress signaling. *Am J Obstet Gynecol*. 2014;211(541):e541–8.
- Salimi A, Nikoosiar Jahromi M, Pourahmad J. Maternal exposure causes mitochondrial dysfunction in brain, liver, and heart of mouse fetus: an explanation for perfluorooctanoic acid induced abortion and developmental toxicity. *Environ Toxicol*. 2019;34:878–85.
- Schulze PC, Yoshioka J, Takahashi T, He Z, King GL, Lee RT. Hyperglycemia promotes oxidative stress through inhibition of thioredoxin function by thioredoxin-interacting protein. *J Biol Chem*. 2004;279:30369–74.
- Houshmand-Oeregaard A, Hjort L, Kelstrup L, et al. DNA methylation and gene expression of TXNIP in adult offspring of women with diabetes in pregnancy. *PLoS One*. 2017;12:e0187038.
- Giacco F, Brownlee M. Oxidative stress and diabetic complications. *Circ Res*. 2010;107:1058–70.
- Wang K, Chen B, Yin T, et al. N-Methylparoxetine blocked autophagic flux and induced apoptosis by activating ROS-MAPK pathway in non-small cell lung cancer cells. *Int J Mol Sci*. 2019;20:3415.
- Li J, Yue Z, Xiong W, Sun P, You K, Wang J. TXNIP overexpression suppresses proliferation and induces apoptosis in SMMC7221 cells through ROS generation and MAPK pathway activation. *Oncol Rep*. 2017;37:3369–76.
- Zheng S, Li X, Zhang Y, et al. PEG-nanolized ultra-small selenium nanoparticles overcome drug resistance in hepatocellular carcinoma HepG2 cells through induction of mitochondria dysfunction. *Int J Nanomed*. 2012;7:3939–49.

16. Liu J, Pang Y, Chen J, et al. Hyperbranched polydiselenide as a self assembling broad spectrum anticancer agent. *Biomaterials*. 2012;33:7765–74.
17. Danz ED, Skramsted J, Henry N, Bennett JA, Keller RS. Resveratrol prevents doxorubicin cardiotoxicity through mitochondrial stabilization and the Sirt1 pathway. *Free Radic Biol Med*. 2009;46:1589–97.
18. Cox NJ. Maternal component in NIDDM transmission. How large an effect? *Diabetes*. 1994;43:166–8.
19. Pettitt DJ, Aleck KA, Baird HR, Carraher MJ, Bennett PH, Knowler WC. Congenital susceptibility to NIDDM. Role of intrauterine environment. *Diabetes*. 1988;37:622–8.
20. Kuhl C. Etiology and pathogenesis of gestational diabetes. *Diabetes Care*. 1998;21(Suppl 2):B19–26.
21. Jauniaux E, Poston L, Burton GJ. Placental-related diseases of pregnancy: involvement of oxidative stress and implications in human evolution. *Hum Reprod Update*. 2006;12:747–55.
22. Osmond DT, Nolan CJ, King RG, Brennecke SP, Gude NM. Effects of gestational diabetes on human placental glucose uptake, transfer, and utilisation. *Diabetologia*. 2000;43:576–82.
23. Stanirowski PJ, Szukiewicz D, Pyzlak M, Abdalla N, Sawicki W, Cendrowski K. Impact of pre-gestational and gestational diabetes mellitus on the expression of glucose transporters GLUT-1, GLUT-4 and GLUT-9 in human term placenta. *Endocrine*. 2017;55:799–808.
24. Jansson T, Wennergren M, Powell TL. Placental glucose transport and GLUT 1 expression in insulin-dependent diabetes. *Am J Obstet Gynecol*. 1999;180:163–8.
25. Jansson T, Myatt L, Powell TL. The role of trophoblast nutrient and ion transporters in the development of pregnancy complications and adult disease. *Curr Vasc Pharmacol*. 2009;7:521–33.
26. Vo T, Hardy DB. Molecular mechanisms underlying the fetal programming of adult disease. *J Cell Commun Signal*. 2012;6:139–53.
27. Gaither K, Quraishi AN, Illsley NP. Diabetes alters the expression and activity of the human placental GLUT1 glucose transporter. *J Clin Endocrinol Metab*. 1999;84:695–701.
28. Muralimanoharan S, Maloyan A, Myatt L. Mitochondrial function and glucose metabolism in the placenta with gestational diabetes mellitus: role of miR-143. *Clin Sci (Lond)*. 2016;130:931–41.
29. International Association of Diabetes and Pregnancy Study Groups, Metzger BE, Gabbe SG, et al. International association of diabetes and pregnancy study groups recommendations on the diagnosis and classification of hyperglycemia in pregnancy. *Diabetes Care*. 2010;33:676–82.
30. Longtine MS, Nelson DM. Placental dysfunction and fetal programming: the importance of placental size, shape, histopathology, and molecular composition. *Semin Reprod Med*. 2011;29:187–96.
31. Kajantie E, Thornburg KL, Eriksson JG, Osmond C, Barker DJ. In preeclampsia, the placenta grows slowly along its minor axis. *Int J Dev Biol*. 2010;54:469–73.
32. Aramesh MR, Dehdashtian M, Malekian A, ShahAli S, Shojaei K. Relation between fetal anthropometric parameters and cord blood adiponectin and high-sensitivity C-reactive protein in gestational diabetes mellitus. *Arch Endocrinol Metab*. 2017;61:228–32.
33. Brownlee M. Biochemistry and molecular cell biology of diabetic complications. *Nature*. 2001;414:813–20.
34. Houstis N, Rosen ED, Lander ES. Reactive oxygen species have a causal role in multiple forms of insulin resistance. *Nature*. 2006;440:944–8.
35. Devi TS, Yumnamcha T, Yao F, Somayajulu M, Kowluru RA, Singh LP. TXNIP mediates high glucose-induced mitophagic flux and lysosome enlargement in human retinal pigment epithelial cells. *Biol Open*. 2019;8:bio038521.
36. Devi TS, Somayajulu M, Kowluru RA, Singh LP. TXNIP regulates mitophagy in retinal Muller cells under high-glucose conditions: implications for diabetic retinopathy. *Cell Death Dis*. 2017;8:e2777.
37. Kinalski M, Sledziewski A, Telejko B, et al. Lipid peroxidation, antioxidant defence and acid-base status in cord blood at birth: the influence of diabetes. *Horm Metab Res*. 2001;33:227–31.
38. Shalev A, Pise-Masison CA, Radonovich M, et al. Oligonucleotide microarray analysis of intact human pancreatic islets: identification of glucose-responsive genes and a highly regulated TGFbeta signaling pathway. *Endocrinology*. 2002;143:3695–8.
39. Sferruzzi-Perri AN, Higgins JS, Vaughan OR, Murray AJ, Fowden AL. Placental mitochondria adapt developmentally and in response to hypoxia to support fetal growth. *Proc Natl Acad Sci USA*. 2019;116:1621–6.
40. Mele J, Muralimanoharan S, Maloyan A, Myatt L. Impaired mitochondrial function in human

- placenta with increased maternal adiposity. *Am J Physiol Endocrinol Metab.* 2014;307:E419–25.
41. Boyle KE, Newsom SA, Janssen RC, Lappas M, Friedman JE. Skeletal muscle MnSOD, mitochondrial complex II, and SIRT3 enzyme activities are decreased in maternal obesity during human pregnancy and gestational diabetes mellitus. *J Clin Endocrinol Metab.* 2013;98:E1601–9.
  42. Ramirez-Emiliano J, Fajardo-Araujo ME, Zuniga-Trujillo I, Perez-Vazquez V, Sandoval-Salazar C, Ornelas-Vazquez JK. Mitochondrial content, oxidative, and nitrosative stress in human full-term placentas with gestational diabetes mellitus. *Reprod Biol Endocrinol.* 2017;15:26.
  43. Mando C, Anelli GM, Novielli C, et al. Impact of obesity and hyperglycemia on placental mitochondria. *Oxid Med Cell Longev.* 2018;2018:2378189.
  44. Holland O, Dekker Nitert M, Gallo LA, Vejzovic M, Fisher JJ, Perkins AV. Review: placental mitochondrial function and structure in gestational disorders. *Placenta.* 2017;54:2–9.
  45. Mando C, De Palma C, Stampalija T, et al. Placental mitochondrial content and function in intrauterine growth restriction and preeclampsia. *Am J Physiol Endocrinol Metab.* 2014;306:E404–13.
  46. Novielli C, Mando C, Tabano S, et al. Mitochondrial DNA content and methylation in fetal cord blood of pregnancies with placental insufficiency. *Placenta.* 2017;55:63–70.
  47. Lee HC, Yin PH, Lu CY, Chi CW, Wei YH. Increase of mitochondria and mitochondrial DNA in response to oxidative stress in human cells. *Biochem J.* 2000;348(Pt 2):425–32.
  48. Pustovrh C, Jawerbaum A, Sinner D, et al. Membrane-type matrix metalloproteinase-9 activity in placental tissue from patients with pre-existing and gestational diabetes mellitus. *Reprod Fertil Dev.* 2000;12:269–75.
  49. Saitoh T, Tanaka S, Koike T. Rapid induction and Ca(2+) influx-mediated suppression of vitamin D3 up-regulated protein 1 (VDUP1) mRNA in cerebellar granule neurons undergoing apoptosis. *J Neurochem.* 2001;78:1267–76.
  50. Chen J, Jing G, Xu G, Shalev A. Thioredoxin-interacting protein stimulates its own expression via a positive feedback loop. *Mol Endocrinol.* 2014;28:674–80.
  51. Mathis D, Vence L, Benoist C.  $\beta$ -Cell death during progression to diabetes. *Nature.* 2001;414:792–8.
  52. Zielonka J, Srinivasan S, Hardy M, et al. Cytochrome c-mediated oxidation of hydroethidine and mito-hydroethidine in mitochondria: identification of homo- and heterodimers. *Free Radic Biol Med.* 2008;44:835–46.
  53. Dikalov SI, Harrison DG. Methods for detection of mitochondrial and cellular reactive oxygen species. *Antioxid Redox Signal.* 2014;20:372–82.
  54. Watson AL, Skepper JN, Jauniaux E, Burton GJ. Susceptibility of human placental syncytiotrophoblastic mitochondria to oxygen-mediated damage in relation to gestational age. *J Clin Endocrinol Metab.* 1998;83:1697–705.
  55. Aouache R, Biquard L, Vaiman D, Miralles F. Oxidative stress in preeclampsia and placental diseases. *Int J Mol Sci.* 2018;19:1496.
  56. Belkacemi L, Lash GE, Macdonald-Goodfellow SK, Caldwell JD, Graham CH. Inhibition of human trophoblast invasiveness by high glucose concentrations. *J Clin Endocrinol Metab.* 2005;90:4846–51.
  57. Singh LP, Devi TS, Yumnamcha T. The role of Txnip in mitophagy dysregulation and inflammasome activation in diabetic retinopathy: a new perspective. *JOJ Ophthalmol.* 2017. <https://doi.org/10.19080/jojo.2017.04.555643>.
  58. Lee Y, Kim KR, McKeon F, et al. A unifying concept of trophoblastic differentiation and malignancy defined by biomarker expression. *Hum Pathol.* 2007;38:1003–13.
  59. Brownbill P, Mahendran D, Owen D, et al. Denudations as paracellular routes for alphafetoprotein and creatinine across the human syncytiotrophoblast. *Am J Physiol Regul Integr Comp Physiol.* 2000;278:R677–83.
  60. Rampersad R, Barton A, Sadovsky Y, Nelson DM. The C5b-9 membrane attack complex of complement activation localizes to villous trophoblast injury in vivo and modulates human trophoblast function in vitro. *Placenta.* 2008;29:855–61.
  61. Sibley CP, Brownbill P, Dilworth M, Glazier JD. Review: adaptation in placental nutrient supply to meet fetal growth demand: implications for programming. *Placenta.* 2010;31(Suppl):S70–4.
  62. Trist BG, Davies KM, Cottam V, et al. Amyotrophic lateral sclerosis-like superoxide dismutase 1 proteinopathy is associated with neuronal loss in Parkinson's disease brain. *Acta Neuropathol.* 2017;134:113–27.

63. Van Damme P, Robberecht W, Van Den Bosch L. Modelling amyotrophic lateral sclerosis: progress and possibilities. *Dis Model Mech*. 2017;10:537–49.
64. Huang L, Ying H, Chen Z, et al. Down-regulation of DKK1 and Wnt1/beta-catenin pathway by increased homeobox B7 resulted in cell differentiation suppression of intrauterine fetal growth retardation in human placenta. *Placenta*. 2019;80:27–35.
65. Lee X, Keith JC Jr, Stumm N, et al. Downregulation of placental syncytin expression and abnormal protein localization in pre-eclampsia. *Placenta*. 2001;22:808–12.
66. Yoshihara E, Masaki S, Matsuo Y, Chen Z, Tian H, Yodoi J. Thioredoxin/Txnip: redoxisome, as a redox switch for the pathogenesis of diseases. *Front Immunol*. 2014;4:514.
67. Li X, Rong Y, Zhang M, et al. Up-regulation of thioredoxin interacting protein (Txnip) by p38 MAPK and FOXO1 contributes to the impaired thioredoxin activity and increased ROS in glucose-treated endothelial cells. *Biochem Biophys Res Commun*. 2009;381:660–5.
68. Woods LC, Berbusse GW, Naylor K. Microtubules are essential for mitochondrial dynamics-fission, fusion, and motility-in dictyostelium discoideum. *Front Cell Dev Biol*. 2016;4:19.
69. Larsen TD, Sabey KH, Knutson AJ, et al. Diabetic pregnancy and maternal high-fat diet impair mitochondrial dynamism in the developing fetal rat heart by sex-specific mechanisms. *Int J Mol Sci*. 2019;20:3090.